ELECTROMAGNETIC FIELD DISTRIBUTION IN THE FAR-FIELD OF A PYRAMIDAL HORN ANTENNA

Robert POPA
Military Technical Academy „Ferdinand I", Bucharest, Romania (rbrtpopa@yahoo.com)
ORCID: 0009-0001-6675-0360

Gheorghe IUBU
Military Technical Academy „Ferdinand I", Bucharest, Romania (gh.iubu@gmail.com)

DOI: 10.19062/1842-9238.2022.20.2.5

Abstract: *The analysis of electromagnetic compatibility problems in radio electronic systems also involves the study of the distribution of the electromagnetic field generated by the antenna system of the device in the far-field area. Having a solid critical overview of the current research on the topic as a starting point, this article presents, in a synthetic, coherent and accessible manner, the procedure for the mathematical modelling of the electromagnetic field radiated in the far-field zone by a pyramidal horn antenna. The second part of the article presents the numerical and graphical results obtained by modelling the procedure described above by means of computer-assisted modelling.*

Keywords: *horn antenna, directivity function, directivity characteristic, opening angle of the directivity characteristic, maximum value of the directivity coefficient, electromagnetic compatibility.*

1. INTRODUCTION

The antenna system of any radio electronic equipment provides the interface of this equipment with the external medium of propagation of the electromagnetic field. The main function of this system is to transform, spatially directive and frequency-selective, when transmitting - the energy of high-frequency currents into the energy of electromagnetic waves, and vice versa, when receiving - the energy of electromagnetic waves into high-frequency currents.

The geometric fundamentals and notations used in the field of antenna theory for Cartesian and spherical coordinate systems are shown in Fig.1 [Balanis], where:

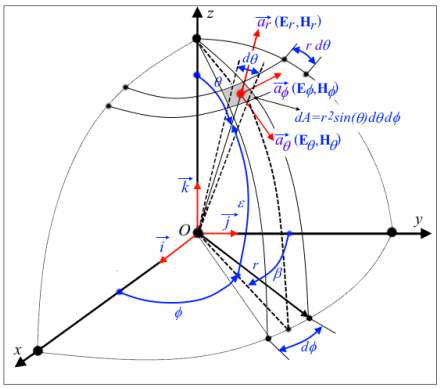

FIG. 1 Geometric foundations for the coordinate system and the notations used

- ϕ is the *azimuthal angle* and $\beta = \pi/2 - \phi$ the complementary angle;
- θ is the *polar angle* and $\varepsilon = \pi/2 - \theta$ the complementary angle called *the elevation angle*;
- $\left(\vec{i}, \vec{j}, \vec{k}\right)$, $\left|\vec{i}\right|^2 + \left|\vec{j}\right|^2 + \left|\vec{k}\right|^2 = 1$, the versors of the Cartesian coordinate system Oxyz;
- $\left(\overrightarrow{a_r}, \overrightarrow{a_\phi}, \overrightarrow{a_\theta}\right)$, $\left|\overrightarrow{a_r}\right|^2 + \left|\overrightarrow{a_\phi}\right|^2 + \left|\overrightarrow{a_\theta}\right|^2 = 1$, the versors of the spherical coordinate system;
- $\left(E_r, E_\phi, E_\theta\right)$, the electric field components in spherical coordinates. For the far field area ($2 \cdot \pi \cdot r/\lambda \gg 1$) $E_r \cong 0$;
- ,$\left(H_r, H_\phi, H_\theta\right)$ the magnetic field components in spherical coordinates. For the far field area $H_r \cong 0$;
- $dA = r^2 \cdot \sin(\theta) \cdot d\phi \cdot d\theta$, the area element in spherical coordinates;
- $d\Omega = dA/r^2 = \sin(\theta) \cdot d\phi \cdot d\theta$, the solid angle element in spherical coordinates;
- $k = \frac{2 \cdot \pi}{\lambda}$, the wave number.

2. FUNDAMENTAL ISSUES REGARDING THE DIRECTIVITY OF ANTENNAS

Any antenna radiates spherical waves that propagate in the radial direction in a coordinate system originating at the point of antenna placement. At large distances, spherical waves can be approximated as plane waves, this approximation being very useful because it simplifies many of the problems related to the mathematical modelling of an antenna.

If $\vec{\mathbf{E}}$ and $\overrightarrow{\mathbf{H}}$ are the orthogonal vectors that describe the values of the electric field intensity and the magnetic field intensity radiated by an antenna, related by the wave impedance in free space $\eta \cong 377\,\Omega$, *the power density* of the radiated electromagnetic wave *or the radiated power per unit area* is described by the modulus of the Poynting vector [16]:

$$S = \left|\vec{\mathbf{S}}\right| = \left|\vec{\mathbf{E}} \times \overrightarrow{\mathbf{H}^*}\right| = \frac{|E|^2}{2 \cdot \eta} = \frac{\eta}{2} \cdot |H|^2 \left[W/m^2\right]. \tag{1}$$

The *electric field strength* radiated by an antenna in the far-field region can be written as $E(r, \phi, \theta) = E^o(\phi, \theta) \cdot \frac{e^{-j \cdot k \cdot r}}{r}$, $E^o(\phi, \theta)$ being the distance independent component. Consequently, the expression of the radiated power density for the far-field region can be written as:

$$S(r, \phi, \theta) = \frac{\left|E(r, \phi, \theta)\right|^2}{2 \cdot \eta} = \frac{1}{r^2} \cdot \frac{\left|E^o(\phi, \theta)\right|^2}{2 \cdot \eta} =$$

$$= \frac{1}{r^2} \cdot \frac{1}{2 \cdot \eta} \cdot \left[\left|E_\theta^o(\phi, \theta)\right|^2 + \left|E_\phi^o(\phi, \theta)\right|^2 + \underbrace{\left|E_r^o(\phi, \theta)\right|^2}_{\gg 0 \text{ far field}} \right] \tag{2}$$

where, with $\left(E_\theta^o, E_\phi^o, E_r^o\right)$ denoted the radiated electric field components, independent of distance, represented in spherical coordinates. If $S \cdot dA$ is the power radiated by the surface element $dA = r^2 \cdot d\Omega$ where $d\Omega$ is the solid angle element in spherical coordinates, it can be written that $S \cdot dA = S \cdot r^2 \cdot d\Omega$.

The value $S(r,\phi,\theta) \cdot r^2 \square U(\phi,\theta)$ is called *the radiation intensity*, being dependent only on the direction of the radiated electromagnetic wave. The radiation intensity can be said to be the radiated power per unit solid angle (the unit of measurement is $W/steradian$). Based on relation (2) we obtain:

$$U(\phi,\theta) = r^2 \cdot S(r,\phi,\theta) = \frac{\left|E^o(\phi,\theta)\right|^2}{2 \cdot \eta} \cong \frac{1}{2 \cdot \eta}\left[\left|E_\theta^o(\phi,\theta)\right|^2 + \left|E_\phi^o(\phi,\theta)\right|^2\right].$$
$$U(\phi,\theta) \cong \frac{\eta}{2}\left[\left|H_\theta^o(\phi,\theta)\right|^2 + \left|H_\phi^o(\phi,\theta)\right|^2\right]. \quad (3)$$

If we denote by U_o the maximum value of the radiation intensity, it can be written:

$$U(\phi,\theta) = U_o \cdot F^2(\phi,\theta). \quad (4)$$

The function $F^2(\phi,\theta)$ describes the angular or spatial distribution of the radiation intensity and is called *the directivity function*, being also called *the power directivity function*. The directivity function itself is $F(\phi,\theta)$ and describes the angular or spatial distribution of the field strength, electric or magnetic. If $(\phi_{\max},\theta_{\max})$ are the angles at which this function reaches its maximum value, $F_{\max} = F(\phi_{\max},\theta_{\max})$, the function $F_n(\phi,\theta) = F(\phi,\theta)/F(\phi_{\max},\theta_{\max})$ is called *the normed directivity function*.

The directivity characteristic or *radiation characteristic* is the graphical representation of the directivity function. This can be represented on a linear scale or on a logarithmic scale (in dB), the latter allowing the secondary lobes to be highlighted. Also, the directivity characteristic can be represented by:

- 2D graphics, in sections $\phi = ct.$ or $\theta = ct.$, in Cartesian coordinates or in polar coordinates, on a linear, linear-logarithmic or logarithmic scale (in dB). The most important sections are $\phi = \phi_{\max} = ct.$ and $\theta = \theta_{\max} = ct.$;
- 3D graphics, in Cartesian coordinates ($\phi \to x$, $\theta \to y$, $F(\phi,\theta) \to z$), in spherical coordinates ($F(\phi,\theta) \cdot \sin(\theta) \cdot \cos(\phi) \to x$, $F(\phi,\theta) \cdot \sin(\theta) \cdot \sin(\phi) \to y$, $F(\phi,\theta) \cdot \cos(\theta) \to z$), on a linear or log scale (in dB).

In the specialized literature consulted [1] we found three-dimensional graphic representations of the directivity characteristic represented in sections, without giving explanations on the procedure used. In Fig. 2 graphically presents the calculation procedure found and used by the author of the article as well as its result, obtained according to the following calculation algorithm and graphic representation: $\theta \cdot \cos(\phi) \to x$, $\theta \cdot \sin(\phi) \to y$, $F_n(\phi,\theta) \to z$, if angles are expressed in radians or $\theta \cdot \cos(\phi \cdot \pi/180) \to x$, $\theta \cdot \sin(\phi \cdot \pi/180) \to y$, $F_n(\phi \cdot \pi/180, \theta \cdot \pi/180) \to z$, if the angles are expressed in degrees.

The most important parameters of the directivity of an antenna or antenna network are related to the shape of the directivity characteristic, respectively:

- ✓ *the opening angles at half power* refer to the opening angles, in the azimuthal plane - $\Delta\phi_{3dB}$ and in the elevation plane - $\Delta\theta_{3dB}$, of the main lobe of the directivity characteristic normalized at the level of half of the maximum radiated power;

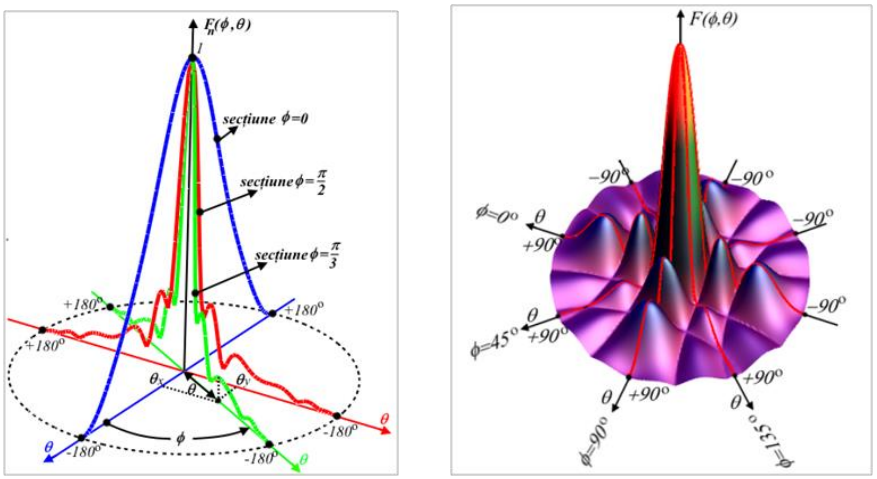

FIG. 2 Section $\phi = ct., 0 \le \phi < 180^\circ$ through the directivity characteristic, in 3D representation

- ✓ *the directivity coefficient* of the antenna is defined as the ratio between the radiation intensity $U(\phi,\theta)$ for a given direction and radiation intensity if the antenna would radiate the same power as an isotropic radiator (a solid angle equal to $4\cdot\pi$) [1]:

$$D(\phi,\theta) = \frac{U(\phi,\theta)}{U_{iso}} = 4\cdot\pi\cdot\frac{F_n^2(\phi,\theta)}{\int_0^{2\cdot\pi}\int_0^{\pi} F_n^2(\phi,\theta)\cdot\sin(\theta)\cdot d\theta\cdot d\phi}. \quad (5)$$

If the direction is not specified, the term *maximum value of the directivity coefficient* is used [1]:

$$D_o = D(\phi_{\max},\theta_{\max}) = \frac{4\cdot\pi}{\int_0^{2\cdot\pi}\int_0^{\pi} F_n^2(\phi,\theta)\cdot\sin(\theta)\cdot d\theta\cdot d\phi}; \quad (6)$$

- ✓ *the distribution and level of the secondary lobes* of the directivity characteristic.

3. MATHEMATICAL MODELLING OF THE ELECTROMAGNETIC FIELD RADIATED BY A PYRAMIDAL HORN ANTENNA

The horn antenna is one of the most widely used antennas, especially in the microwave field, either as an independent antenna or as a primary source in reflector antennas, equipping radio communication systems, radar systems or systems intended for radio astronomy. Also, some modern radio electronic systems using phased antenna arrays use the horn antenna as their elemental antenna. Its widespread applicability is determined by its constructional simplicity, ease of powering, versatility, and relatively high gain [1].

Depending on the opening of the radiating surface, horn antennas can have a rectangular opening or a conical opening. Horn antennas whose aperture is obtained by

widening (flaring) in a plane a rectangular waveguide are also called sector horn E, if the widening occurs in the E plane, or sector horn H, if the broadening occurs in the H plane. If the widening occurs in both planes, a pyramidal horn antenna is obtained (Fig. 3).

The meaning of the notations in the figure and the connection relationships between the geometric parameters of the pyramid horn antenna are:

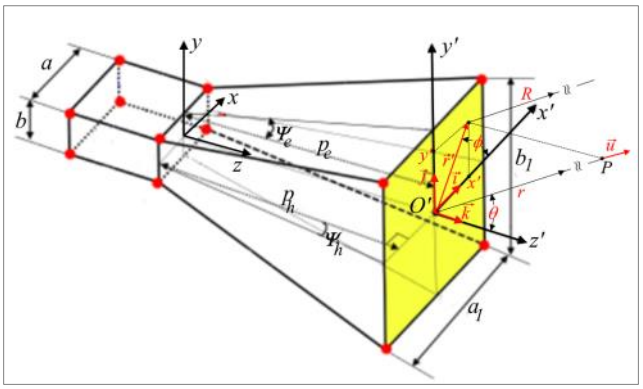

a) three-dimensional view

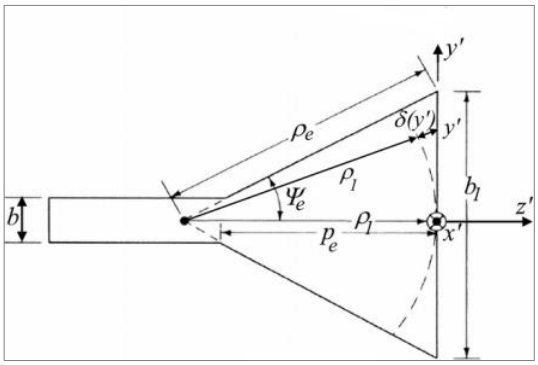

b) E plane view

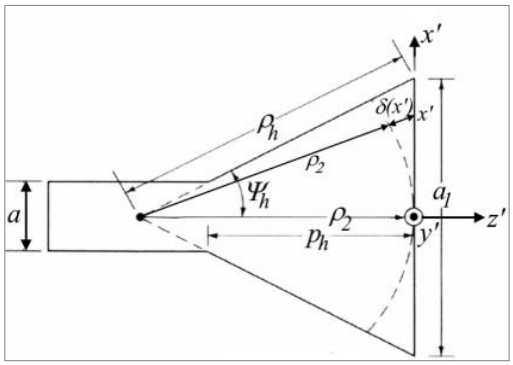

c) H plane view

FIG. 3 Pyramidal horn configuration *[1]*

- the opening semi-angles in the plans E and H, respectively Ψ_e and Ψ_h:

$$\psi_e = \text{arctg}\left[b_1/(2\cdot\rho_1)\right],\ \psi_h = \text{arctg}\left[a_1/(2\cdot\rho_2)\right]. \quad (7)$$

The values b_1, a_1 characterize the opening of the horn antenna and ρ_1, ρ_2 the radii of the circular arcs of equal phase, in the H and E planes. Normalized to the wavelength, these quantities are denoted by: $b_{1n} = b_1/\lambda, a_{1n} = a_1/\lambda, \rho_{1n} = \rho_1/\lambda, \rho_{2n} = \rho_2/\lambda$;

- the heights p_e, p_h of the trapezoidal sections in planes E and H:

$$p_e = \rho_1 - b/\left[2\cdot\tan(\psi_e)\right],\ p_h = \rho_2 - a/2\cdot\tan(\psi_h). \quad (8)$$

The condition of physical realization of the horn imposes the equality of the heights of the chimney in the two planes: $p_e = p_h$;

- $\vec{\mathbf{u}} = u_x\cdot\vec{i} + u_y\cdot\vec{j} + u_z\cdot\vec{k} = \sin(\theta)\cdot\cos(\phi)\cdot\vec{i} + \sin(\theta)\cdot\sin(\phi)\cdot\vec{j} + \cos(\theta)\cdot\vec{k}$ is the versor of the normal to the wavefront in the far-field region;
- $\vec{\mathbf{r}}' = x'\cdot\vec{i} + y'\cdot\vec{j}$ is the position vector of a point in the horn antenna aperture.

3.1 The procedure for evaluating the directivity function expression

In order to determine the expression of the directivity function of the pyramid horn antenna, it is necessary to go through several stages of calculation. Without going into the details of the proofs, the procedure for evaluating the expression of the directivity function of the pyramid horn antenna, assumes [1]:

1) *determining the distribution of components* $\overrightarrow{\mathbf{E}'}, \overrightarrow{\mathbf{H}'}$ *of the electromagnetic field* in the horn antenna opening (plane $x'O'y'$). There are many laborious mathematical models for determining the field distribution in the horn antenna opening. A fairly accurate model, described in the paper [Balanis], starts from the assumption of the field distribution in the opening of the funnel feeding waveguide described by the mode TE_{10}. At a point in the opening of the horn antenna, characterized by the position vector $\overrightarrow{\mathbf{r}'} = x' \cdot \vec{i} + y' \cdot \vec{j}$, this field is out of phase with respect to the centre of the horn opening $(x' = y' = 0)$ due to road differences $\delta(x'), \delta(y')$ (Fig. 3 b), 3c):

$$E_y'(x', y') = E_o \cdot \cos\left(\frac{\pi}{a_1} \cdot x'\right) e^{-j \cdot k \cdot \left[\delta(x') + \delta(y')\right]},\ H_x'(x', y') = -E_y'(x', y')/\eta\,. \tag{9}$$

The path differences can be roughly deduced from the equalities:

$$\begin{aligned} &\rho_1^2 + y'^2 = \left[\rho_1 + \delta(y')\right]^2 = \rho_1^2 + 2 \cdot \rho_1 \cdot \delta(y') + \underbrace{\delta^2(y')}_{\approx 0} \Rightarrow \boxed{\delta(y') \approx \frac{1}{2} \frac{y'^2}{\rho_1}}, \\ &\rho_2^2 + x'^2 = \left[\rho_2 + \delta(x')\right]^2 = \rho_2^2 + 2 \cdot \rho_2 \cdot \delta(x') + \underbrace{\delta^2(x')}_{\approx 0} \Rightarrow \boxed{\delta(x') \approx \frac{1}{2} \frac{x'^2}{\rho_2}}. \end{aligned} \tag{10}$$

As a result, the approximate field components described by (9) become:

$$E_y'(x', y') \approx E_o \cdot \cos\left(\frac{\pi}{a_1} \cdot x'\right) e^{-j \cdot \frac{k}{2} \cdot \left[\frac{x'^2}{\rho_2} + \frac{y'^2}{\rho_1}\right]},\ H_x'(x', y') \approx -E_y'(x', y')/\eta\,. \tag{11}$$

2) *determination of equivalent electric current density expressions* $\mathbf{J}'_s$ and *equivalent magnetic current density* $\mathbf{M}'_s$, from the opening of the radiant surface:

$$\begin{aligned} &\mathbf{J}'_s = \mathbf{n} \times \mathbf{H} = \vec{k} \times \vec{i} \cdot H_x'(x', y') \approx -\vec{j} \cdot \frac{E_o}{\eta} \cos\left(\frac{\pi}{a_1} \cdot x'\right) e^{-j \cdot \frac{k}{2} \cdot \left[\frac{x'^2}{\rho_2} + \frac{y'^2}{\rho_1}\right]} = \vec{j} \cdot J_y(x', y'), \\ &\mathbf{M}'_s = -\mathbf{n} \times \mathbf{E} = -\vec{k} \times \vec{j} \cdot E_y'(x', y') \approx \vec{i} \cdot E_o \cdot \cos\left(\frac{\pi}{a_1} \cdot x'\right) e^{-j \cdot \frac{k}{2} \cdot \left[\frac{x'^2}{\rho_2} + \frac{y'^2}{\rho_1}\right]} = \vec{i} \cdot M_x(x', y'). \end{aligned} \tag{12}$$

3) *conversion of vector components* $\mathbf{J}'_s = \vec{i} \cdot J_x + \vec{j} \cdot J_y + \vec{k} \cdot J_z = \vec{j} \cdot J_y$ and $\mathbf{M}'_s = \vec{i} \cdot M_x + \vec{j} \cdot M_y + \vec{k} \cdot M_z = \vec{i} \cdot M_x$, from Cartesian coordinates to spherical coordinates using the matrix relation:

$$\begin{pmatrix} A_r \\ A_\theta \\ A_\phi \end{pmatrix} = \begin{pmatrix} \sin(\theta) \cdot \cos(\phi) & \sin(\theta) \cdot \sin(\phi) & \cos(\theta) \\ \cos(\theta) \cdot \cos(\phi) & \cos(\theta) \cdot \sin(\phi) & -\sin(\theta) \\ -\sin(\phi) & c\cos(\phi) & 0 \end{pmatrix} \cdot \begin{pmatrix} A_x \\ A_y \\ A_z \end{pmatrix}. \tag{13}$$

Finally, it is obtained that:

$$\begin{aligned}\mathbf{J}'_s(x',y',\phi,\theta)&=\left[\overrightarrow{a_r}\cdot\sin(\theta)\cdot\sin(\phi)+\overrightarrow{a_\theta}\cdot\cos(\theta)\cdot\sin(\phi)+\overrightarrow{a_\phi}\cdot\cos(\phi)\right]\cdot J_y(x',y')\\ \mathbf{M}'_s(x',y',\phi,\theta)&=\left[\overrightarrow{a_r}\cdot\sin(\theta)\cdot\cos(\phi)+\overrightarrow{a_\theta}\cdot\cos(\theta)\cdot\cos(\phi)-\overrightarrow{a_\phi}\cdot\sin(\phi)\right]\cdot M_x(x',y').\end{aligned} \tag{14}$$

4) determination of *the magnetic potential vector* **A** produced by the electric current density $\mathbf{J}'_s$ and of *the electric potential vector* **F** produced by the magnetic current density $\mathbf{M}'_s$ in the far field zone:

$$\mathbf{A}(r,\phi,\theta)=\frac{\mu}{4\cdot\pi}\cdot\iint_{S'}\mathbf{J}(x',y',\phi,\theta)\cdot\frac{e^{-j\cdot k\cdot R}}{R}\cdot ds', \tag{15}$$

$$\mathbf{F}(r,\phi,\theta)=\frac{\varepsilon}{4\cdot\pi}\cdot\iint_{S'}\mathbf{M}'_s(x',y',\phi,\theta)\cdot\frac{e^{-j\cdot k\cdot R}}{R}\cdot ds'. \tag{16}$$

From Fig. 3. a) it follows that

$$R=r-\Delta r=r-\underset{\Delta r}{\overrightarrow{r'}\cdot\vec{u}}=r-\underbrace{\left[x'\cdot\sin(\theta)\cdot\cos(\phi)+y'\cdot\sin(\theta)\cdot\sin(\phi)\right]}_{\Delta r}.$$

Influence of path difference Δr on the amplitude being negligible and having an effect only on the phase, with the area element $ds'=dx'\cdot dy'$, the relations (15) and (16) becomes:

$$\mathbf{A}(r,\phi,\theta)=\frac{\mu}{4\cdot\pi}\cdot\frac{e^{-j\cdot k\cdot r}}{r}\cdot\mathbf{N}(\phi,\theta), \tag{17}$$

with

$$\mathbf{N}(\phi,\theta)=\int_{-a_1/2}^{+a_1/2}\int_{-b_1/2}^{+b_1/2}\mathbf{J}'_s(x',y',\phi,\theta)\cdot e^{-j\cdot k\cdot\left[x'\cdot\sin(\theta)\cdot\cos(\phi)+y'\cdot\sin(\theta)\cdot\sin(\phi)\right]}dx'\cdot dy' \tag{17-a}$$

and

$$\mathbf{F}(r,\phi,\theta)=\frac{\varepsilon}{4\cdot\pi}\cdot\frac{e^{-j\cdot k\cdot r}}{r}\cdot\mathbf{L}(\phi,\theta), \tag{18}$$

with

$$\mathbf{L}(\phi,\theta)=\int_{-a_1/2}^{+a_1/2}\int_{-b_1/2}^{+b_1/2}\mathbf{M}'_s(x',y',\phi,\theta)\cdot e^{-j\cdot k\cdot\left[x'\cdot\sin(\theta)\cdot\cos(\phi)+y'\cdot\sin(\theta)\cdot\sin(\phi)\right]}dx'\cdot dy' \tag{18-a}$$

Based on relations (14), separating from relations (17-a) and (18-a) the components of versors $\overrightarrow{a_\phi}$, $\overrightarrow{a_\theta}$

$$\begin{aligned}N_\phi(\phi,\theta)&=-(E_o/\eta)\cdot\cos(\phi)\cdot I_1(\phi,\theta)\cdot I_2(\phi,\theta)\\ N_\theta(\phi,\theta)&=-(E_o/\eta)\cdot\cos(\theta)\cdot\sin(\phi)\cdot I_1(\phi,\theta)\cdot I_2(\phi,\theta),\\ L_\phi(\phi,\theta)&=-E_o\cdot\sin(\phi)\cdot I_1(\phi,\theta)\cdot I_2(\phi,\theta)\\ L_\theta(\phi,\theta)&=E_o\cdot\cos(\theta)\cdot\cos(\phi)\cdot I_1(\phi,\theta)\cdot I_2(\phi,\theta),\end{aligned} \tag{19}$$

in which:

$$I_1(\phi,\theta)=\int_{-a_1/2}^{+a_1/2}\cos\left(\frac{\pi}{a_1}x'\right)\cdot e^{-j\cdot k\cdot\left[x'^2/2\rho_2-x'\cdot\sin(\theta)\cdot\cos(\phi)\right]}\cdot dx', \tag{20}$$

(2)

$$I_2(\phi,\theta)=\int_{-b_1/2}^{+b_1/2} e^{-j\cdot k\cdot\left[y'^2/(2\rho_1)-y'\cdot\sin(\theta)\cdot\sin(\phi)\right]}\cdot dy'.$$

With the notations:

$$\begin{aligned}
t_1(\phi,\theta)&=\sqrt{2\cdot\rho_{1n}}\cdot\left[-\mathrm{tg}(\Psi_e)-\sin(\theta)\cdot\sin(\phi)\right],\\
t_2(\phi,\theta)&=\sqrt{2\cdot\rho_{1n}}\cdot\left[\mathrm{tg}(\Psi_e)-\sin(\theta)\cdot\sin(\phi)\right],
\end{aligned}\tag{3}$$

$$\begin{aligned}
t_1'(\phi,\theta)&=\sqrt{2\cdot\rho_{2n}}\cdot\left[-\mathrm{tg}(\Psi_h)-\sin(\theta)\cdot\cos(\phi)-1/(2\cdot a_{1n})\right],\\
t_2'(\phi,\theta)&=\sqrt{2\cdot\rho_{2n}}\cdot\left[\mathrm{tg}(\Psi_h)-\sin(\theta)\cdot\cos(\phi)-1/(2\cdot a_{1n})\right],
\end{aligned}\tag{22-a}$$

$$\begin{aligned}
t_1''(\phi,\theta)&=\sqrt{2\cdot\rho_{2n}}\cdot\left[-\mathrm{tg}(\Psi_h)-\sin(\theta)\cdot\cos(\phi)+1/(2\cdot a_{1n})\right],\\
t_2''(\phi,\theta)&=\sqrt{2\cdot\rho_{2n}}\cdot\left[\mathrm{tg}(\Psi_h)-\sin(\theta)\cdot\cos(\phi)+1/(2\cdot a_{1n})\right],
\end{aligned}\tag{22-b}$$

$$\begin{aligned}
f_1(\phi,\theta)&=\pi\cdot\rho_{2n}\cdot\left[\sin(\theta)\cdot\cos(\phi)+1/(2\cdot a_{1n})\right]^2,\\
f_2(\phi,\theta)&=\pi\cdot\rho_{2n}\cdot\left[\sin(\theta)\cdot\cos(\phi)-1/(2\cdot a_{1n})\right]^2,\\
f_3(\phi,\theta)&=\pi\cdot\rho_{1n}\cdot\left[\sin(\theta)\cdot\sin(\phi)\right]^2,
\end{aligned}\tag{22-c}$$

is obtained:

$$\begin{aligned}
I_1(\phi,\theta)=\frac{\lambda}{2}\sqrt{\frac{\rho_{2n}}{2}}\cdot\Big\{&e^{j\cdot f_1(\phi,\theta)}\cdot C\left[t_1'(\phi,\theta),t_2'(\phi,\theta)\right]+\\
&+e^{j\cdot f_2(\phi,\theta)}\cdot C\left[t_1''(\phi,\theta),t_2''(\phi,\theta)\right]\Big\}=\lambda\cdot I_{1n}(\phi,\theta)
\end{aligned}\tag{4}$$

$$I_2(\phi,\theta)=\lambda\cdot\sqrt{\frac{\rho_{1n}}{2}}\cdot e^{j\cdot f_3(\phi,\theta)}\cdot C\left[t_1(\phi,\theta),t_2(\phi,\theta)\right]=\lambda\cdot I_{2n}(\phi,\theta).\tag{5}$$

The function $C(x,y)$ is defined as $C(x,y)\equiv C_F(y)-C_F(x)-j\cdot\left[S_F(y)-S_F(x)\right]$ where C_F, S_F represent the Fresnel integrals.

5) determination of *field intensity expressions* in the far-field region:

$E_r(r,\phi,\theta)\equiv 0$, $H_r(r,\phi,\theta)\equiv 0$,

$$\begin{aligned}
E_\theta(r,\phi,\theta)&=-j\cdot\frac{k\cdot e^{-j\cdot k\cdot r}}{4\cdot\pi\cdot r}\cdot\left[L_\phi(\phi,\theta)+\eta\cdot N_\theta(\phi,\theta)\right],\\
E_\phi(r,\phi,\theta)&=+j\cdot\frac{k\cdot e^{-j\cdot k\cdot r}}{4\cdot\pi\cdot r}\cdot\left[L_\phi(\phi,\theta)-\eta\cdot N_\theta(\phi,\theta)\right],\\
H_\theta(r,\phi,\theta)&=-j\cdot\frac{k\cdot e^{-j\cdot k\cdot r}}{4\cdot\pi\cdot r}\cdot\frac{1}{\eta}\cdot\left[L_\phi(\phi,\theta)-\eta\cdot N_\theta(\phi,\theta)\right],\\
H_\phi(r.\phi,\theta)&=-j\cdot\frac{k\cdot e^{-j\cdot k\cdot r}}{4\cdot\pi\cdot r}\cdot\frac{1}{\eta}\cdot\left[L_\phi(\phi,\theta)+\eta\cdot N_\theta(\phi,\theta)\right].
\end{aligned}\tag{6}$$

The electric field intensity in the far-field region of the pyramidal horn radiator is obtained by vector summation of the components $\overrightarrow{E_\phi(r,\theta,\phi)}$ and $\overrightarrow{E_\theta(r,\theta,\phi)}$, respectively $\overrightarrow{E(r,\theta,\phi)}=E_\phi(r,\theta,\phi)\cdot\overrightarrow{a_\phi}+E_\theta(r,\theta,\phi)\cdot\overrightarrow{a_\theta}$.

Based on relations (25), for the components of the electric field $\overrightarrow{E_\phi(r,\theta,\phi)}$ and $\overrightarrow{E_\theta(r,\theta,\phi)}$ in the far field area, is obtained:

$$E_\phi(r,\theta,\phi)=\frac{\lambda}{r}\cdot e^{-j\cdot k\cdot r}\cdot\underbrace{\left(j\cdot\frac{E_o}{2}\right)\cdot\left\{\cos(\phi)\cdot\left[\cos(\theta)+1\right]\cdot I_{1n}(\theta,\phi)\cdot I_{2n}(\theta,\phi)\right\}}_{E_\phi^o(\phi,\theta)}= \tag{26}$$

$$=\frac{\lambda}{r}\cdot e^{-j\cdot k\cdot r}\cdot E_\phi^o(\phi,\theta)$$

$$E_\theta(r,\theta,\phi)=\frac{\lambda}{r}\cdot e^{-j\cdot k\cdot r}\cdot\underbrace{\left(j\cdot\frac{E_o}{2}\right)\cdot\left\{\sin(\phi)\cdot\left[\cos(\theta)+1\right]\cdot I_{1n}(\theta,\phi)\cdot I_{2n}(\theta,\phi)\right\}}_{E_\theta^o(\phi,\theta)}= \tag{27}$$

$$=\frac{\lambda}{r}\cdot e^{-j\cdot k\cdot r}\cdot E_\theta^o(\phi,\theta).$$

Therefore

$$\overrightarrow{E(r,\phi,\theta)}=\underbrace{\left[E_\phi^o(\phi,\theta)\cdot\overrightarrow{a_\phi}+E_\phi^o(\phi,\theta)\cdot\overrightarrow{a_\theta}\right]}_{\overrightarrow{E_o(\phi,\theta)}}\cdot\frac{\lambda}{r}\cdot e^{-j\cdot k\cdot r}=\frac{\lambda}{r}\cdot e^{-j\cdot k\cdot r}\cdot\overrightarrow{E_o(\phi,\theta)} \tag{7}$$

where $\overrightarrow{E_0(\phi,\theta)}$ is the distance-independent component of the electric field:

$$\overrightarrow{E_o(\phi,\theta)}=E_\phi^o(\phi,\theta)\cdot\overrightarrow{a_\phi}+E_\phi^o(\phi,\theta)\cdot\overrightarrow{a_\theta}=$$

$$=\left(j\cdot\frac{E_o}{2}\right)\cdot\left\{\left[\cos(\theta)+1\right]\cdot I_{1n}(\theta,\phi)\cdot I_{2n}(\theta,\phi)\right\}\cdot\left[\cos(\phi)\cdot\overrightarrow{a_\phi}+\sin(\phi)\cdot\overrightarrow{a_\theta}\right]. \tag{29}$$

The module of this component is:

$$E_o(\phi,\theta)=\left|E_\phi^o(\phi,\theta)\cdot\overrightarrow{a_\phi}+E_\phi^o(\phi,\theta)\cdot\overrightarrow{a_\theta}\right|=$$

$$=E_o\cdot\underbrace{\frac{1}{2}\left\{\left[\cos(\theta)+1\right]\cdot I_{1n}(\theta,\phi)\cdot I_{2n}(\theta,\phi)\right\}}_{F_h(\phi,\theta)}\cdot\overbrace{\left[\cos^2(\phi)+\sin^2(\phi)\right]}^{1}=E_o\cdot F_h(\phi,\theta), \tag{30}$$

where $F_h(\phi,\theta)$ is ***the directivity function of the pyramid horn antenna***:

$$\boxed{F_h(\phi,\theta)=\frac{1}{2}\cdot\left[1+\cos(\theta)\right]\cdot I_{1n}(\phi,\theta)\cdot I_{2n}(\phi,\theta)} \tag{8}$$

The maximum value of this function is obtained for zero values of the angular coordinates (ϕ,θ):

$$\boxed{\left|F_h(0,0)\right|=F_{\max}=\left|I_{1n}(0,0)\cdot I_{2n}(0,0)\right|.} \tag{9}$$

3.2 The analysis of the maximum value of the directivity coefficient

The maximum value of the directivity coefficient of the pyramid horn antenna can be calculated with the relation [1]:

$$D_{o\_hp}=8\cdot\pi\cdot\frac{\rho_{1n}\cdot\rho_{2n}}{a_{1n}\cdot b_{1n}}\cdot\left|C(u,v)\right|^2\cdot\left[C_F^2(w)+S_F^2(w)\right], \tag{33}$$

$$\mathrm{u}=\frac{1}{\sqrt{2}}\left(\frac{\sqrt{\rho_{2n}}}{a_{1n}}+\frac{a_{1n}}{\sqrt{\rho_{2n}}}\right),\ \mathrm{v}=\frac{1}{\sqrt{2}}\left(\frac{\sqrt{\rho_{2n}}}{a_{1n}}-\frac{a_{1n}}{\sqrt{\rho_{2n}}}\right),\ w=\frac{b_{1n}}{\sqrt{2\cdot\rho_{1n}}} \tag{10}$$

.

Having seen that [1]

$$D_{o\_hE} = \frac{64}{\pi} \cdot \frac{a_n \cdot \rho_{1n}}{b_{1n}} \cdot \left| C_F^2(w) + S_F^2(w) \right|, \tag{11}$$

$$D_{o\_hH} = \frac{\pi}{32} \cdot \frac{b_n \cdot \rho_{2n}}{a_{1n}} \cdot \left| C(u,v) \right|^2 \tag{12}$$

represent the expressions of *the maximum values of the directivity coefficients of the sectoral horn antennas*, in planes E and H, relation (33) can be written:

$$D_{o\_hp} = \frac{\pi}{32} \cdot \frac{1}{a_n \cdot b_n} \cdot D_{o\_hE} \cdot D_{o\_hH} \cdot \tag{13}$$

Maximizing value D_{o_hp} is equivalent to maximizing values D_{o_hE} and D_{o_hH}. The values of the coefficients D_{o_hE} and D_{o_hH} each depends only on the parameters that characterize the opening of the horn in planes E or H. In Fig. 4 shows the dependence of the maximum value of the directivity coefficient on the antenna parameters, for the sectoral horn antennas, in the E and H planes. It is found that, in the case of the sectoral horn E, for a value ρ_{1n} given the height at the apex, normed at λ, there is an optimal value b_{1n} of the antenna opening in the plane E that maximizes the value of the directivity coefficient:

$$b_{1n\_opt} = \sqrt{2 \cdot \rho_{1n}} \tag{14}$$

Similarly, for a sector horn antenna in the H plane,

$$a_{1n\_opt} = \sqrt{3 \cdot \rho_{2n}} \tag{15}$$

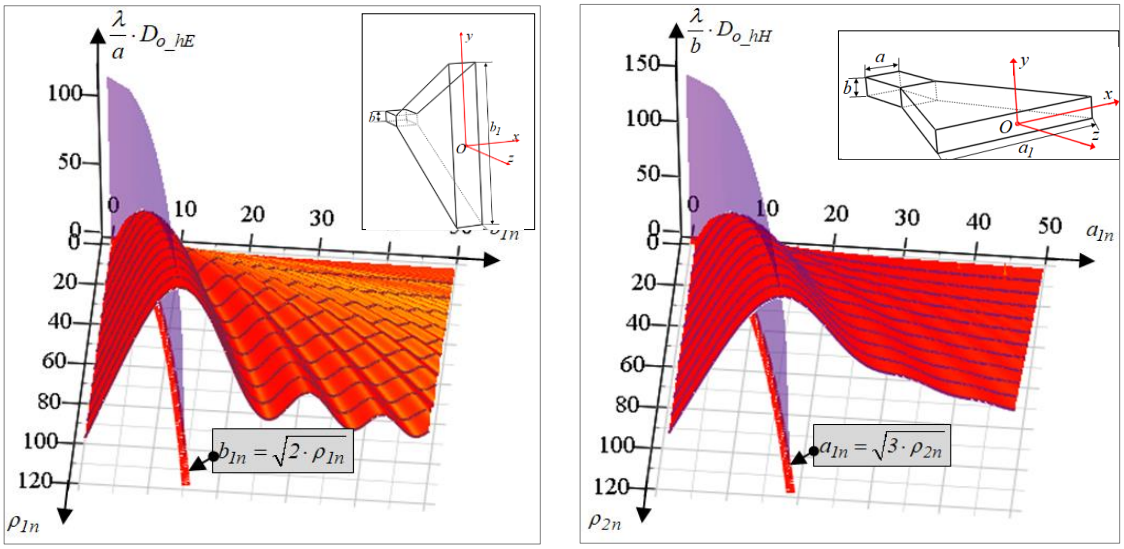

a) sectoral horn, E plane b) sectoral horn, H plane

FIG. 4 Dependence on the antenna parameters of the maximum value of the directivity coefficient, for sector horn antennas

For these values, $u = \frac{1}{\sqrt{2}}\left(\frac{1}{\sqrt{3}} + \sqrt{3}\right)$, $v = \frac{1}{\sqrt{2}}\left(\frac{1}{\sqrt{3}} - \sqrt{3}\right)$, $w = 1$ and the optimal expression of the maximum value of the directivity coefficient of the pyramid horn antenna is:

$$D_{o\_hp\_opt} = 15.83 \cdot \sqrt{\rho_{1n} \cdot \rho_{2n}} \ . \tag{40}$$

Fulfillment of the physical feasibility condition $p_e = p_h \Leftrightarrow \rho_1 \left(1 - \frac{b}{b_1}\right) = \rho_2 \left(1 - \frac{a}{a_1}\right)$ but also of conditions (38) and (39), impose the following relationship between the optimal apertures of the pyramidal horn antenna, normalized to λ:

$$a_{1n\_opt} = \frac{a_n + \sqrt{a_n^2 + 6 \cdot b_{1n\_opt} \cdot \left(b_{1n\_opt} - b_n\right)}}{2} \tag{41}$$

The maximum value of the directivity coefficient can also be determined based on the directivity function, using relations (6), (31) and (32) and the numerical evaluation of the integrals. The differences are not greater than 0.25 dbs.

4. RESULTS OBTAINED THROUGH COMPUTER MODELLING

Based on the mathematical formalism presented above, a program was created in MATHCAD to evaluate, numerically and graphically, the performance of the directivity of a pyramid horn antenna.

With the help of library functions of the programming environment and functions built by the programmer, the program allows:

- ✓ calculation and graphic representation of the most important parameters of the directivity of the pyramidal horn antenna:
  - calculation of the directivity function;
  - graphic plotting of the directivity characteristic, in sections, in Cartesian coordinates, polar/spherical coordinates, on a linear scale or a logarithmic scale in dB;
  - graphic plotting of the directivity characteristic in spherical coordinates (3D format), on a linear or logarithmic scale in dB;
  - visualization of the directivity characteristic represented in spherical coordinates, together with the geometric sketch of the pyramid horn antenna that has this characteristic;
  - calculation of the opening angles at -3 dB of the main lobe of the directivity characteristic, in two planes – the azimuthal plane (H) and the elevation plane (E);
  - calculation of the maximum value of the directivity coefficient;
- ✓ the generation of models of numerical calculation functions and graphics generators not included in the programming environment but which, through the generality of the arguments, help the development of the calculation program but also the understanding of the obtained graphic representations:
  - the decibel conversion function for graphical representation on a logarithmic scale in spherical coordinates;
  - functions for calculating the opening angles at -3 dB of the main lobe of the directivity characteristic, in two planes – the azimuthal plane (H) and the elevation plane (E);
  - the function of generating and 3D graphic representation of scaled geometric sketches of modelled chimney antennas;
  - functions for generating the axes of the Cartesian coordinate system, the axes and circle arcs for 3D delimitation of the opening level at -3dB of the directivity characteristics;

- calculation functions and graphic plotting of spherical caps intended to delimit the different levels of the characteristics represented in spherical coordinates, on a logarithmic scale in dbs.

The results obtained for a working frequency $f_o = 2{,}5\,GHz \Leftrightarrow \lambda = 12\,cm$ are presented below.

To begin with, based on the geometric model presented in Fig. 5.a, the coordinates of the peaks, the parametric equations of its sides and axes were defined ($N_v = 12$ peaks, $N_l = 20$ sides and $N_a = 3$ axes). These elements were introduced into the program and generated the representation in Fig. 5b.

The calculation performed by the program for the maximum value of the directivity function of the pyramid horn antenna returns the result: $F_{max} = F_h(0,0) = 7.71$.

Opening angles at - 3dB of the main lobe of the directivity characteristic of the pyramidal horn antenna for the sections $\phi = 0$, respectively $\phi = \pi/2$, were evaluated with the "root" function available in Mathcad:

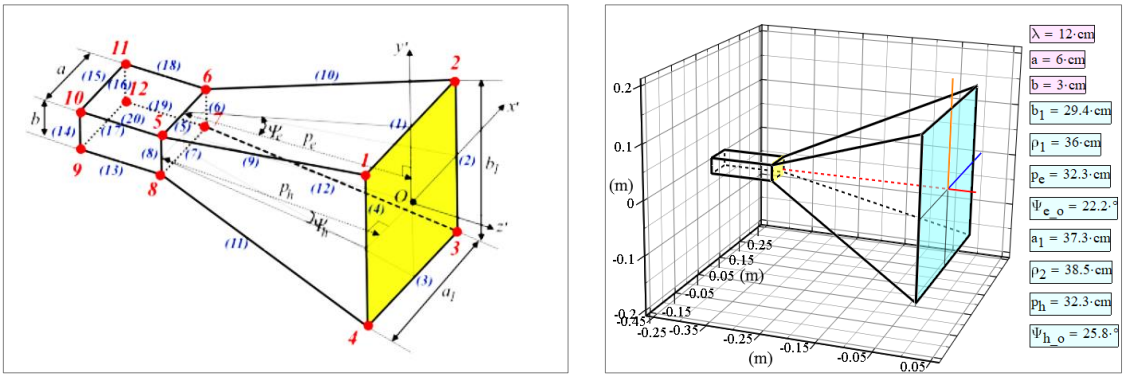

a) the structure of the geometric model of the pyramid horn antenna

b) scale sketch of pyramidal horn antenna

FIG. 5 The geometric model used and the sketch of the pyramid horn antenna drawn to scale

$$\Delta\theta_{hH\_3dB} = 2 \cdot root\left[F_h(0,\theta) - \frac{\sqrt{2}}{2} \cdot F_{max}, \theta, 0, \pi\right] = 24.8^o; \tag{16}$$

$$\Delta\theta_{hE\_3dB} = 2 \cdot root\left[F_h\left(\frac{\pi}{2},\theta\right) - \frac{\sqrt{2}}{2} \cdot F_{max}, \theta, 0, \pi\right] = 21.8^o \tag{17}$$

The maximum value of the directivity coefficient calculated based on relations (33) and (34) is $D_{o\_hp} = 49.1\,(16.91\,dB)$ and the one obtained based on relation (6), using approximate calculation methods of integrals, is $D_{o\_hp} = 50{,}8\,(17.06\,dB)$.

In Fig. 5 ÷ Fig. 7 shows the results of the graphical representations of the directivity characteristic of the pyramid horn antenna, obtained with the program mentioned above.

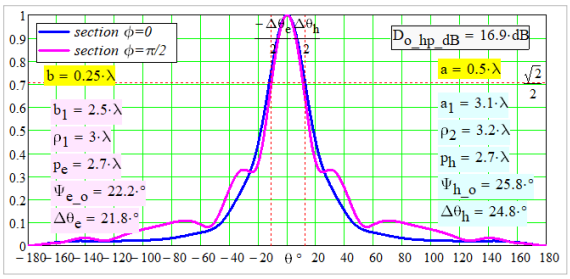

a) Cartesian coordinates, linear scale

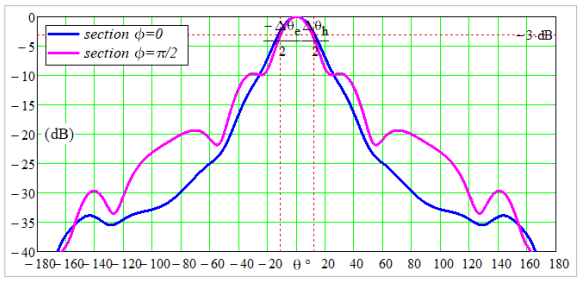

b) Cartesian coordinates, logarithmic scale in dB

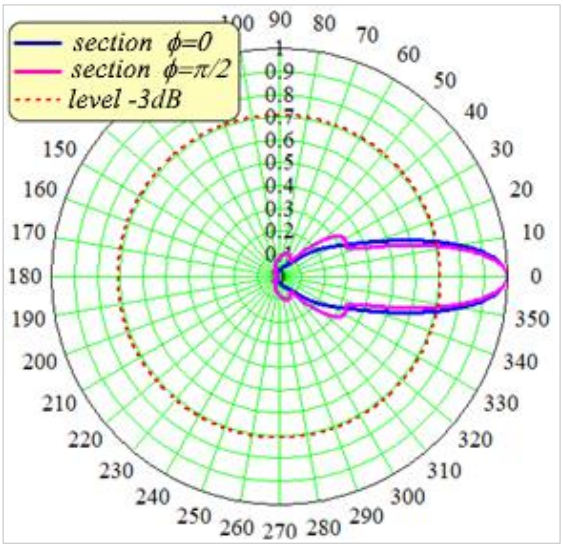

c) polar coordinates, linear scale

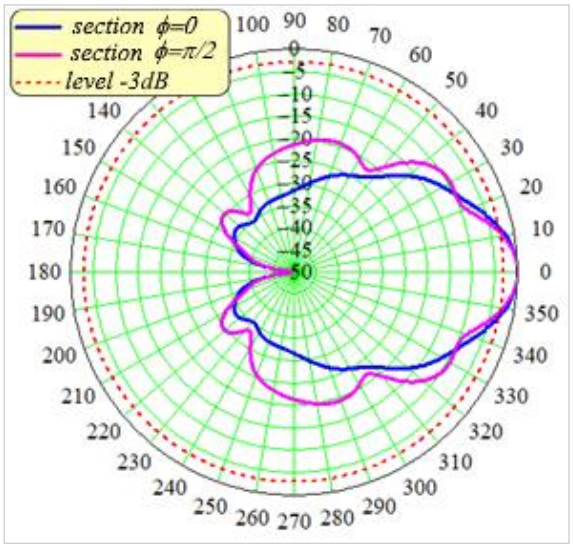

d) polar coordinates, logarithmic scale in dB

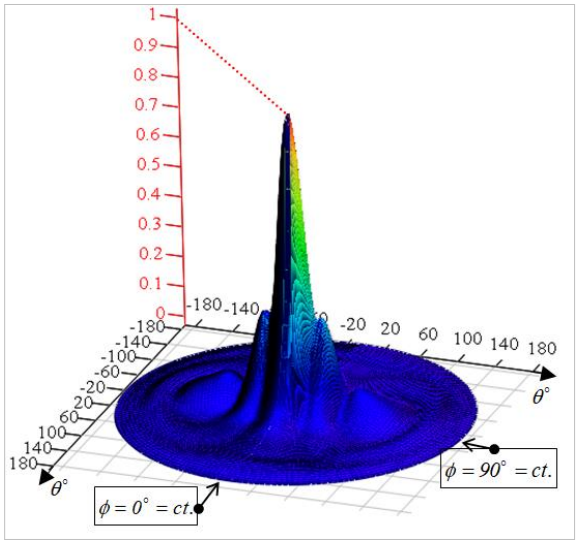

e) sections $\phi = ct.$ in 3D representation, linear scale

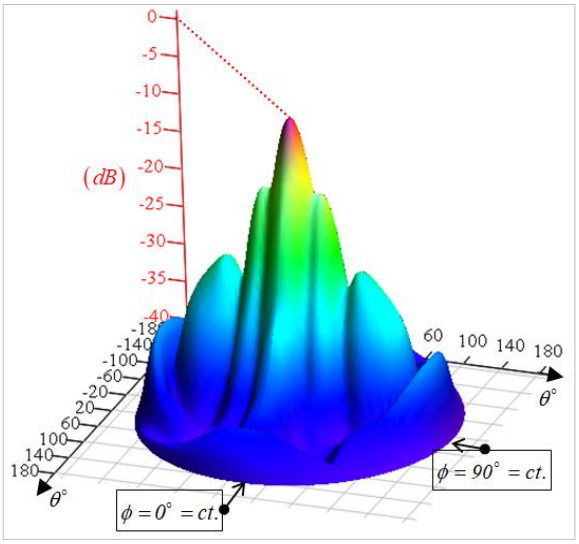

f) sections $\phi = ct.$ in 3D representation, logarithmic scale in dB

FIG. 5 Directivity characteristic of the pyramidal horn antenna in sections $\phi = ct.$

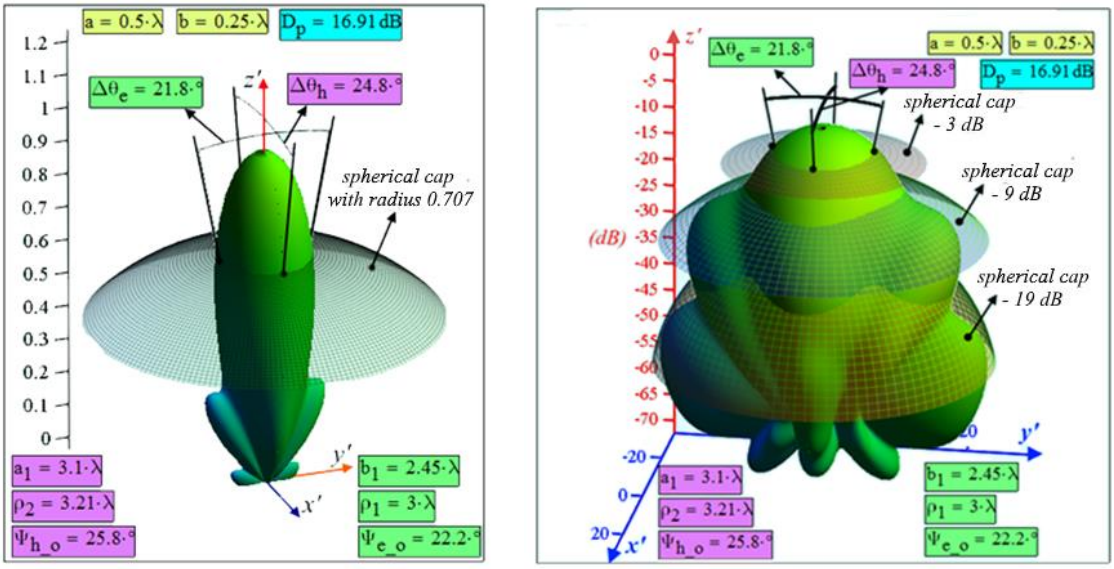

a) linear scale b) logarithmic scale in dB

FIG.6 Representation in spherical coordinates of the directivity characteristic of the pyramid horn antenna

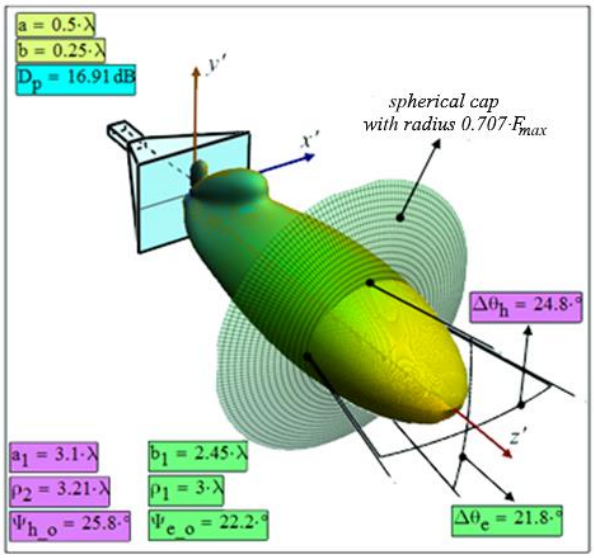

Fig.7 Representation in spherical coordinates - linear scale, of the directivity characteristic of the pyramidal horn antenna together with its scale sketch

5. CONCLUSIONS

The analysis of the obtained results leads to the following conclusions:

- ✓ the absolute value of the electric field and magnetic field intensities generated by a pyramidal horn antenna in the far field area is directly proportional to the module of its directivity function;
- ✓ the shape of the directivity characteristic and the values of the opening angles of its main lobe in planes E and H as well as the maximum value of the directivity coefficient do not depend on the wavelength, being dependent only on the geometric values normalized to the wavelength $b_{1n}, \rho_{1n}, a_{1n}, \rho_{2n}$.

- ✓ for each set of values ρ_{1n}, ρ_{2n} there are optimal values of the horn antenna aperture that maximize the directivity coefficient: $b_{1\_opt} = \sqrt{2\rho_{1n}}$, $a_{1\_opt} = \sqrt{3\rho_{2n}}$;
- ✓ for the modelled configuration, with $\rho_{1n} = 3,\ b_{1n} = b_{1n\_opt} = 2.45,\ \rho_{2n} = 3.21,$ $a_{1n} = a_{1n\_opt} = 3.1$, the values resulted are $\Delta\theta_e = 21.8^\circ$, $\Delta\theta_h = 24.8^\circ$, $D_{o\_hp} = 16.91\,dB$. Also, the directivity characteristic presents a main lobe and several significant secondary lobes, adjacent to the main lobe (without zero crossings), with the level of $-9.7\,dB, -19.4\,dB$ and $-31.2\,dB$.

The shape of the directivity characteristic of the pyramid horn antenna is correlated with its constructive dimensions. Along with the increase in size of the dimensions ρ_1, ρ_2 normalized to the wavelength, the directivity of the horn antenna improves but the phase error between the edge and the centre of the horn increases, the approximations used in relations (10) and (11) which allowed the quadratic approximation of the phase in the opening of the horn antenna and based on which they could Fresnel integrals should be used, requiring possible phase corrections. By calling the numerical integral, however, evaluations of the directivity of the horn antenna can be made, starting from exact expressions of the path differences from relations (10) and (11).

REFERENCES

[1] C. A. Balanis, „*Antenna Theory: Analysis and Design, Fourth Edition*", New York, John Wiley &Sons Publishers, Inc., 2016;

[2] G. Gavrilă, „Complemente de unde electromagnetice", Bucharest, Editura tehnică, 2018;

[3] T. A. Milligan, „*Modern Antenna Design, Second Edition*", Willey-IEEE Press, 2005;

[4] ***IEEE Standard Association, "*IEEE 145-2013 Standard for Definitions of Terms for Antennas*", 11 12 2013. [Online]. Available: https://standards.ieee.org/ieee/145/4705/;

[5] W. L. Stutzman și G. A. Thiele, „*Antenna Theory and Design, Third Edition*", New York, John Wiley & Sons Publishers, Inc., 2012;

[6] S. J. Orfanidis, „*Electromagnetic Waves and Antennas*", Piscataway, New Jersey, Rutgers University, 2016;

[7] ***„*Antenna Engineering Handbook, 5th Edition*", New York, McGraw-Hill Book Company, 2018;

[8] R. E. Collins, „*Antennas and Radiowave Propagation*", New York, New York, McGraw-Hill Book Company, 1985;

[9] N. K. Nikolova, „*Lecture notes on antenna engineering*" 2018. [Interactiv]. Available: http://www.ece.mcmaster.ca/faculty/nikolova/antenna_dload/current_lectures/.